IEEE Access
Multidisciplinary | Rapid Review | Open Access Journal

Received April 13, 2019, accepted May 8, 2019, date of publication May 22, 2019, date of current version June 5, 2019.

Digital Object Identifier 10.1109/ACCESS.2019.2918246

A New Method for Reduction of Atomic Magnetometer Noise Based on Multigene Genetic Programming

WEI QUAN[1,2,3,4], FENG LIU[1], AND WENFENG FAN[1]

[1]School of Instrumentation and Optoelectronic Engineering, Beihang University, Beijing 100191, China
[2]Innovative Research Institute of Frontier Science, Beihang University, Beijing 100191, China
[3]Advanced Innovation Center for Big Data-Based Precision Medicine, Beihang University, Beijing 100191, China
[4]Beijing Academy of Quantum Information Sciences, Beijing 100191, China

Corresponding author: Feng Liu (liufeng1991@buaa.edu.cn)

This work was supported in part by the National Key R&D Program of China under Grant 2016YFB0501600, in part by the Fundamental Research Funds for the Central Universities, in part by the National Natural Science Foundation of China under Grant 61773043, and in part by the National Natural Science Foundation Group of China under Grant 61773043.

ABSTRACT An ultra-high precision magnetic field measurement is of great scientific and economic significance. An atomic magnetometer that operates in a spin-exchange relaxation-free (SERF) regime has superior sensitivity and, thus, is of great significance for the ultra-high precision magnetic field measurement. In order to reduce the noise of a SERF atomic magnetometer and further improve its sensitivity, a method for noise reduction based on the multigene genetic programming (MGGP) is presented. Different from the existing methods, in this method, the model of magnetometer noise is established based on the experimental data. Namely, the noise of the SERF atomic magnetometer is first modeled by the MGGP algorithm and then reduced by the obtained model. Besides, in this way, the sensitivity is improved. The experimental results indicate that our MGGP model can adequately reflect the characteristics of the SERF magnetometer noise. Moreover, after applying the proposed method, the sensitivity of the SERF magnetometer is improved about 13 times at 1 Hz, and there is also a significant sensitivity increase at the frequencies less than 10 Hz. Therefore, the proposed method can effectively reduce the noise and improve the sensitivity of the SERF magnetometer in the low-frequency band.

INDEX TERMS Atomic magnetometer noise modeling, multigene genetic programming, sensitivity improvement, spin-exchange relaxation-free regime.

I. INTRODUCTION

The ultra-high sensitivity magnetic field measurement can be applied to the biomedical science [1], [2], physics [3], magnetic anomaly prospecting [4], [5], and other related fields, providing an important contribution to the scientific research and national economy. The magnetic field measurement device is a core of a magnetic field measurement system, and it defines the sensitivity of magnetic field measurement. Among these devices, the atomic magnetic field measurement device based on the spin-exchange relaxation-free (SERF) theory, which has an extremely high theoretical sensitivity [6], [7] and can theoretically achieve preferable magnetic field measurement sensitivity of 1 $aT/\sqrt{Hz}$ [7], is the basis for future magnetic field measurement instruments with ultra-high sensitivity. In [8], it was reported that devices based on the SERF theory could be utilized in biomedical treatments, electric dipole moment measurements, and charge-parity-time reversal symmetry breaking measurements [3], [6], [9]. Likewise, an atomic magnetometer, which has an extremely high sensitivity, has been extensively applied in the magnetic resonance imaging [10] and magneto-encephalography [11].

According to the report in 2010, the SERF magnetometer can achieve very high sensitivity of 160 $aT/\sqrt{Hz}$ [12]. However, one of the possible approaches to enhance device sensitivity is to decrease noise. There are two main strategies for SERF magnetometer noise reduction. The first one is based

The associate editor coordinating the review of this manuscript and approving it for publication was Mustafa Servet Kiran.

on hardware modifications; for instance, using a low noise magnetic shielding layer [13] and in-situ magnetic compensation considering the probe beam pumping effect [14]. Although such an approach is effective in noise reduction, hardware modification is very costly and time-consuming. Namely, when the magnetic shielding layer is used, there is a magnetic field gradient in the magnetic shield, which leads to the additional gradient broadening; therefore, an effective method to measure the magnetic field gradient is necessary. One such method was presented in [15]. The second strategy for noise reduction is based on software modifications. The software-based noise reduction methods reduce the noise using algorithms which are developed based on equipment noise model. Therefore, compared to the hardware-based methods, the software-based noise reduction methods have lower cost, and their implementation is less time-consuming, which makes them more suitable for practical application.

In recent years, the time series analysis, artificial neural networks, and nonlinear wavelet modeling have been widely used in data modeling. Besides, the time series analysis, including the auto-regressive moving average (ARMA) model has been widely applied to different prediction models. However, the ARMA model can be applied only to smooth and linear data, which makes it inappropriate for nonlinear modeling [16]. Recently, the artificial neural networks (ANNs), the support vector machine (SVM) [17], [18] and some other artificial intelligence (AI) [19] based methods have been declared as powerful computer-based modeling tools. Namely, it was shown that they are more effective in nonlinear modeling than the ARMA model [16]. However, neither ANNs nor SVM can provide an exact mathematical expression of the relationship between input and output variables. In addition, the ANNs require large datasets to establish an appropriate model. In recent years, the genetic programming (GP) algorithms including the multigene genetic programming (MGGP) algorithm (i.e., an improved GP method) have been more and more utilized in nonlinear time series modeling because of numerous advantages. For instance, any form of objective functions and constraints, whether linear or nonlinear, discrete or continuous can be processed by GP, in addition, it is very effective for global search. In [20], it was reported that GP could be applied in modeling and optimization of a random atomic spin gyroscope drift. In addition, in [21] the GP was utilized to lock the distributed feedback laser diode frequency to the gas absorption lines.

The MGGP algorithm is very effective in modeling without any prior knowledge, and it has very high objectivity and versatility. The additional advantage of the MGGP algorithm is that it provides a specific mathematical relationship between input and output data, and can optimize model parameters. Moreover, the MGGP does not require a large amount of data for modeling. Furthermore, the MGGP can be configured to evolve the multigene individuals. Therefore, using the MGGP highly-accurate models can be developed [22].

In this paper, a noise reduction method for SERF magnetometers based on the MGGP model is introduced. First, a model of the SERF magnetometer noise is developed. Next, the SERF magnetometer output signal at no input signal is measured to determine the SERF magnetometer noise. Then, the MGGP algorithm is utilized to establish the model of SERF magnetometer noise. Afterwards, in the magnetic field measurement by a SERF magnetometer, the noise is reduced using the previously developed MGGP noise model. Finally, the sensitivity of SERF magnetometer is improved. The results show that the sensitivity is improved by 13 times at 1 Hz.

The rest of this paper is organized as follows. In Section II presents the proposed method in detail including SERF magnetometer noise, the MGGP algorithm parameters and process and the procedure of SERF magnetometer sensitivity improvement. Section III the experimental setup and result anasys are described. Finally, Section IV concludes the paper.

II. SENSITIVITY INCREASE PRINCIPLE

A. SERF MAGNETOMETER NOISE

The magnetometer model can be expressed as follows:

$$B_{out} = B_{true} + B_{bias} + B_{noise}. \tag{1}$$

where B_{out} denotes the output signal of a SERF magnetometer, B_{true} denotes the true magnetic signal, B_{bias} denotes the systematic error, and B_{noise} represents the SERF magnetometer noise. The noise and bias are the two main factors limiting the magnetometer sensitivity, both of which are time-varying. Therefore, it is of great importance to determine noise and bias values. However, noise consists of different noise types, such as magnetic noise, optical noise electrical noise, and thermal noise. As well known, in a SERF magnetometer, the multiple magnetic shield layers are usually used to provide an extremely weak magnetic environment required to maintain the SERF regime. Namely, several layers of μ-metal can attenuate the external field by many orders of magnitude. However, the sensitivity of a SERF magnetometer is limited by the magnetic noise generated by the innermost layer of the magnetic shield [13]. In particular, magnetic viscosity effects result in an imaginary component of magnetic permeability at a low frequency and generate the magnetization noise with a $1/f$ power spectrum [23]. Following the method for an electrostatic problem involving a charge inside a long, hollow conducting cylinder, the longitudinal magnetic field noise on the shield axis is given by:

$$\delta B_{magn} = \frac{0.26\mu_0}{r\sqrt{t}}\sqrt{\frac{4kT\mu''}{\omega\mu'^2}} \tag{2}$$

where ω denotes the driving angular frequency, μ'' and μ' respectively denote the imaginary and real part of the complex permeability $\mu = \mu' - i\mu''$, r and t are respectively the inner radius and thickness of a shield, T denotes the thermodynamic temperature. Laser noise is another important component of the SERF magnetometer noise. A beam of circularly polarized light is used to pump the atoms, and a linearly polarized light is used for signal detection. Since both

power and frequency of a laser are fluctuating, changes in the pumping rate and optical rotation angle can be caused, which will cause noise generation. Namely, according to the optical rotation theory, the relationship between the optical rotation angle, which is closely related to the magnetic field signal, and laser frequency denotes the Lorentz lines near the atomic resonance peak. Thermal noise is another significant component of the SERF magnetometer noise because the atomic density of the alkali metal cell is directly determined by its temperature. Furthermore, the sensitivity of a SERF magnetometer is also affected by electrical noise in the photoelectric conversion, signal transmission, and so on. In conclusion, there is a complex nonlinear relationship between the magnetometer noise and its components. Therefore, it is difficult to establish a clear analytical model using only the theoretical analysis. On the other hand, the MGGP could be used to model the magnetometer noise using experimental data without a clear understanding of the relationship between the noise and sensitivity.

In this work, the MGGP algorithm is utilized to establish the specific mathematical expressions of measurement noise of a SERF magnetometer and to optimize the coefficients of these mathematical expressions.

B. MGGP MODEL OF MAGNETOMETER NOISE

1) THE MGGP ALGORITHM

At present, the genetic programming methods are much more popular than the conventional linear forecasting methods because they can be model complex nonlinear relationships. In this paper, the MGGP algorithm, which represents an improved GP algorithm, is utilized to establish a model of the SERF magnetometer noise. The MGGP algorithm input data is the magnetometer output signal when there is no applied magnetic field. For the sake of simplicity, in the following, the term 'noise' is used to represent both noise and bias. The MGGP algorithm is a new evolutionary modeling method that aims at finding out a model which presents the relationship between input and output data best. One of the most important advantages of this algorithm is that the model can be developed without any prior knowledge about the structure.

The MGGP algorithm constructs a model with a tree-like structure, whose leaves are called terminals while the other nodes, including the root, are called functions. As shown in Fig.1, the top of a tree-like structure denotes the root, the point where two branches converge denotes a node, and leaves construct the bottom. The elements of terminals are incontrovertible so that the independent variables of a given problem, zero-argument functions, and random constants can be treated as terminals [24]. However, the functions require arguments, which can be arithmetic operators $\{+, -, \times, \div, sin, cos, log, exp, sqrt, square, etc.\}$,, mathematical functions with parameters, conditional statements, or even user-defined operators [25]. For instance, an equation can be expressed as a tree-like structure, where equation elements denote the leaves that are called terminals, and arithmetic operators denote the root and nodes

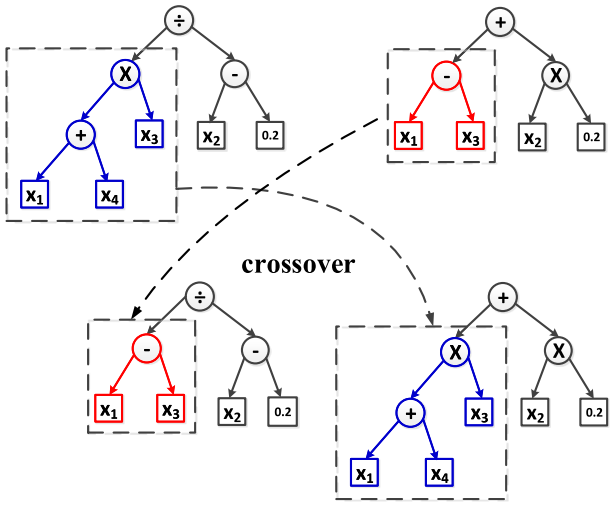

FIGURE 1. The operation of low-level crossover operator.

which are called functions. This method based on the phenomena in evolutionary biology can simultaneously create many different models similarly to many individuals in the biological population. Each model element depends on the functional set and terminal set. Besides, the model structure changes dynamically due to the genetic operations such as crossover, mutation, and reproduction, and in genetics, they are respectively called the hybridization, heredity, and gene mutation. A proper choice of a function set, whose quantity and style determine the MGGP model complexity is very important. A small number of functions in the function set will decrease model accuracy. On the other hand, a large number of functions will expand the explore space and affect the modeling, and even lead to no solution. The MGGP algorithm performs well very on mixed, combinatorial, and many other complex problems. Moreover, the probability of falling into a local optimum is less than for the gradient search method [20]. The MGGP combines the GP ability to select the best model structure with the classical regression ability to estimate the parameter by using a multigene [26]. Every MGGP individual program consists of several traditional GP trees, where each tree can be regarded as a gene, and the overall model represents a weighted linear combination of those genes.

The basic operations of the MGGP algorithm are the crossover, mutation, and reproduction [26], [27]. There are two crossover types in the MGGP algorithm, the first one is a two-point high-level crossover operator which is executed at the gene level, while the other one is a low-level crossover and it is performed at the sub-tree level. When the two-point high-level crossover operator is applied, two individuals in the current population are selected as parents based on their fitness values, and for each parent, two crossover points are set. Then, two offspring are formed by swapping the genes enclosed by the crossover points between the parents. In the case of a low-level crossover operator, a gene is randomly chosen from each parent and branch is selected from each

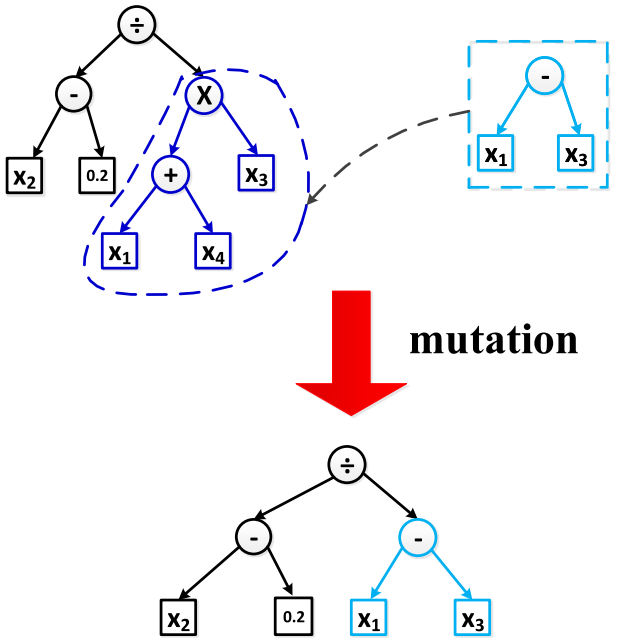

FIGURE 2. The procedure of mutation operation.

gene. Then, two new genes are formed by swapping the two branches. The operation principle of the low-level crossover operator is illustrated in Fig. 1. The mutation, which can be defined as a mutating part randomly chosen from the selected individual of the current population, denotes a genetic operator used to create a new offspring. The high-level mutation merely reshuffles the genes, but the individual structure is un-changed. Hence, the mutation operator works at the sub-tree level in an almost identical manner as its traditional GP counterpart. The mutation operation where a randomly selected node is replaced by a randomly generated GP tree is illustrated in Fig. 2.

The MGGP algorithm represents a very smart AI algorithm which can be used for noise modeling and mitigation of unwanted features, such as time-depended bias. The development of a model is relatively fast, but modeling time-consumption depends on data size. For the data size used in this study, the model-developing process took only decades of seconds. In addition, the MGGP algorithm is an advanced algorithm that does not require a large amount of data to develop the model. However, the larger the data amount is, the more accurate the model will be.

2) THE MGGP ALGORITHM PARAMETERS AND PROCESS

In this paper, the function set F and terminal set T are chosen as follow:

$$F = \{+, -, \times, \div, sin, cos, exp, sqrt, square\}. \quad (3)$$

These symbols are arithmetic operators, and they represent addition, subtraction, multiplication, sine function, cosine function, exponential function, square root, and square functions. To model the nonlinearity, along with addition and subtraction, we also add multiplication, sine function, cosine function, exponential function, square root, and square functions to the function set. These operations are important for model characterization.

$$T = \{x_1, x_2, x_3, x_4, C_0\}. \quad (4)$$

where $X = \{x_1, x_2, x_3, x_4\}$ denotes the set of independent variables, $x_i = B_{signal}(t - i)$ denotes the measurement noise of a SERF magnetometer at the time moment $(t - i)$, where $i = 1, 2, 3, 4$. The SERF magnetometer output at the previous moments contains the variation trend of the noise, so they are chosen as the termination set. In addition, there is a system bias in the magnetometer output signal, so we include a constant C_0 which stands for system bias in the termination set. The initial generation results in a sequence of random tree-like structures that are made up of functions and terminal values. Each tree-like structure is randomly chosen and has both roots and branches. It should be noted that the root set has to be an operator, and it can be randomly chosen only from the function set F. Also, the leaf node has to belong to the terminal set T, and the other non-leaf nodes can be chosen randomly from the union of these sets, $F \bigcup T$. The objective function used in the MGGP model is the minimum deviation. The smaller the deviation between the magnetometer noise calculated by the established model and the measured noise is, the more accurate the established model will be. The main goal is square noise minimization. The least square principle is utilized to design the fitness function, whose simplified expression is given by:

$$F_{fitness} = 1 - \frac{\sum_{i=1}^{n} \left(N_{actual}[i] - N_{forecast}[i]\right)^2}{\sum_{i=1}^{n} \left(N_{actual}[i] - N_{average}\right)^2}. \quad (5)$$

where n denotes the total amount of time-series data, $N_{actual}[i]$ denotes the real output at time moment i^{th}, $N_{forecast}[i]$ denotes the output forecasted by the MGGP model at time moment i^{th}, and $N_{average}$ denotes the mean value of all the actual values of the real output. The denominator is constant if the actual data is specified. Further, the value of $\sum_{i=1}^{n} \left(N_{actual}[i] - N_{forecast}[i]\right)^2$ is correlated with the MGGP model. The higher the model accuracy is, the smaller the fitness function value is. Therefore, it is very reasonable to use a fitness function to measure the efficiency of the MGGP model. The SERF magnetometer model is selected randomly and then modified based on the fitness function value. Next, the algorithm compares the fitness function value of all the selected model. The larger the value is, the better the model is. The inferior model is eliminated, and the better model is selected. After every selection, all selected models are backed to the current generation; models can be selected or copied for many times. After selection, the selected model is modified by the evolutionary operators. The simplest and most useful operators are crossover and mutation. Namely, two models are selected, and one point is taken as a swapping point in the crossover, and each sub-tree from that point is exchanged with some other to create the offspring. The mutation operator

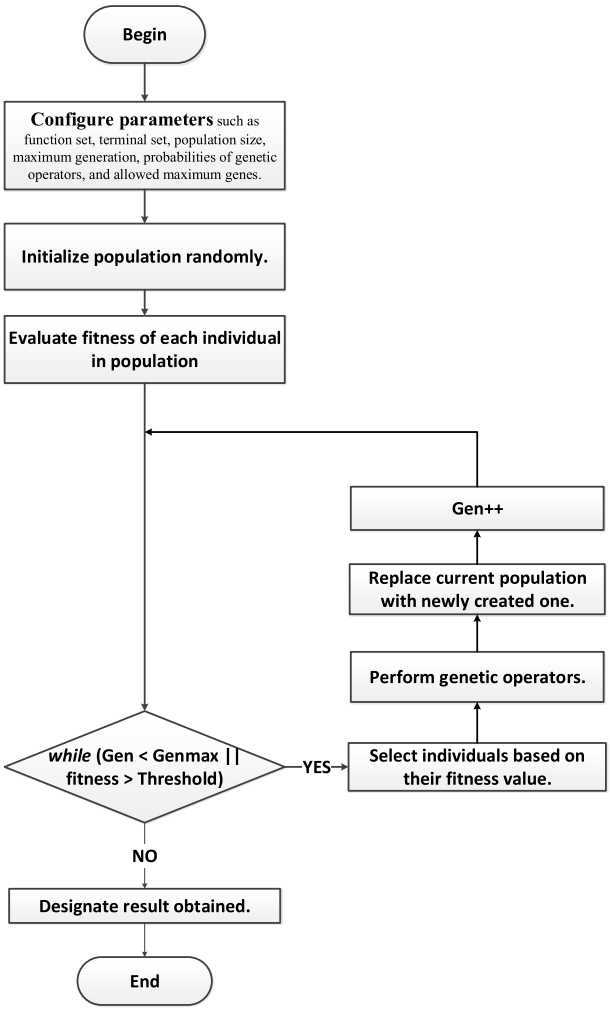

FIGURE 3. The algorithm of MGGP.

is implemented directly. The offspring of a selected gene is moved to the position of its parent by mutation operator. The MGGP algorithm is shown in Fig. 3.

C. SERF MAGNETOMETER SENSITIVITY IMPROVEMENT

The procedure of SERF magnetometer sensitivity improvement is shown in Fig. 4, where it can be seen that SERF magnetometer sensitivity is improved in six steps. In general, a SERF magnetometer outputs electrical signals. Therefore, the magnetometer should be calibrated first, to determine the relationship between the magnetometer output and the calibrated magnetic field. An oscillating field $B_{osc} = B_0 \cos(2\pi ft)$ along the sensitive axis of the SERF magnetometer is generally applied to calibrate a SERF atomic magnetometer [28], where B_0 is the amplitude of the oscillation, and f is the oscillating frequency. In particular, it should be noted that the amplitude of SERF magnetometer output varies with the frequency [28], [29]. The amplitude-frequency response can be fitted by the normalized frequency-response function, which is given by [29]:

$$S_{out}(f) = A\Big/\sqrt{f^2 + B^2} + C \tag{6}$$

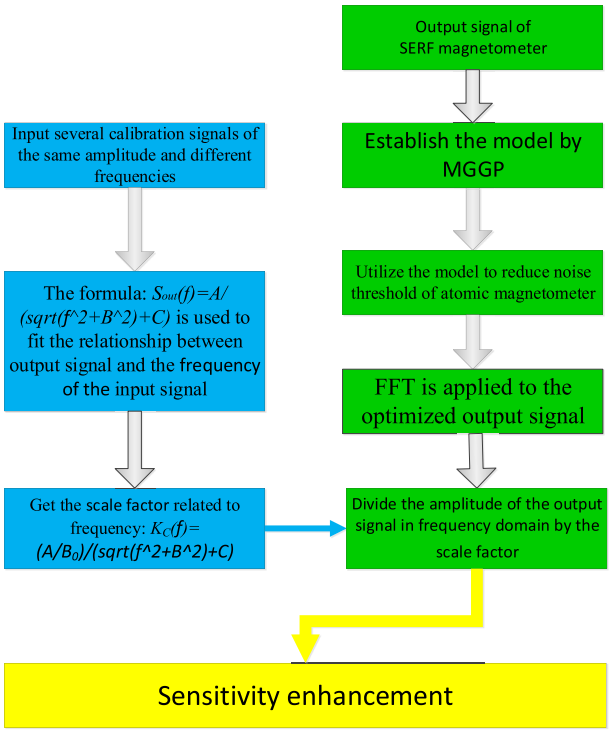

FIGURE 4. The procedure of SERF magnetometer sensitivity improvement.

where S_{out} denotes the amplitude of the SERF atomic magnetometer output signal. Then, the calibration coefficient related to the frequency is expressed as:

$$K_c(f) = A/B_0\Big/\sqrt{f^2 + B^2} + C. \tag{7}$$

Accordingly, the first step (the blue part in Fig. 4) can be divided into three sub-steps: (1) input several calibration signals of the same amplitude and different frequencies; (2) fit the amplitude-frequency response by (6); (3) calculate the scale coefficient by (7). The remaining five steps are shown in the green part, in Fig. 4. The second step relates to the measurement of output signal without a calibration signal, which is regarded as the MGGP training set. The third step is to build a model by using the MGGP algorithm. In the fourth step, the developed model is used to predict the noise at the next moment based on the noise data at the previous four moments, and remove the predicted signal from the real signal, leaving the optimized signal, which is described as reducing the noise threshold. The fifth step is to apply the fast Fourier transform to the optimized signal to obtain the signal amplitude in the frequency domain. The final step is to convert the voltage-amplitude signal in the frequency domain to the SERF magnetometer sensitivity using the calibration coefficient obtained in the first step.

III. EXPERIMENTAL SETUP AND RESULTS ANALYSIS

A. EXPERIMENTAL SETUP

The experimental setup is presented in Fig. 5, wherein it can be seen that it mainly included three parts: SERF atomic

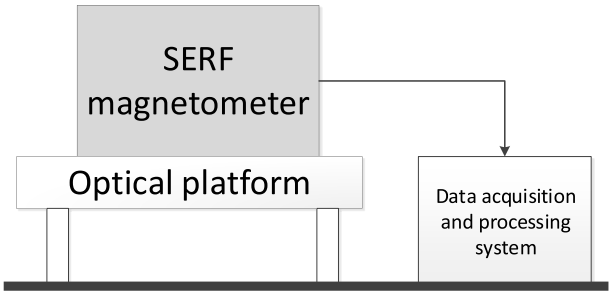

FIGURE 5. The experimental apparatus for SERF magnetometer.

TABLE 1. The frequencies of the ten oscillating field and the amplitude of their corresponding output signals.

Number	Frequency	Amplitude
1	$1Hz$	$920mV$
2	$5Hz$	$911mV$
3	$10Hz$	$880mV$
4	$15Hz$	$840mV$
5	$20Hz$	$779mV$
6	$30Hz$	$682mV$
7	$40Hz$	$591mV$
8	$60Hz$	$468mV$
9	$80Hz$	$380mV$
10	$100Hz$	$322mV$

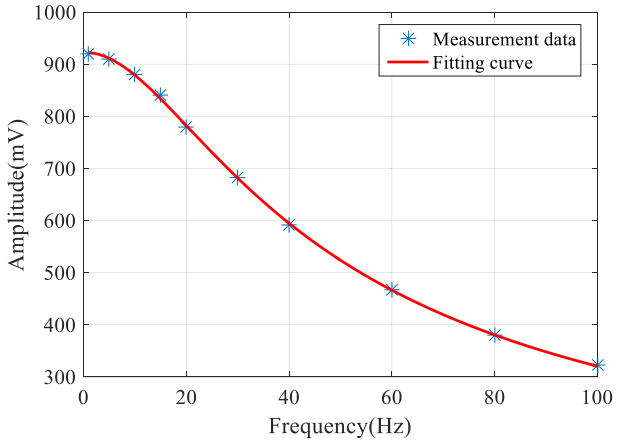

FIGURE 6. The normalized frequency-response function.

TABLE 2. The appropriate parameter settings of MGGP.

Parameter	Value
Population size	100
Maximum number of generation	100
Terminate value	0.003
Tournament size	6
Maximum number of genes	3

magnetometer, optical platform, and data acquisition system. The SERF atomic magnetometer was used to create the original data of the magnetometer. The optical platform served as a support platform of the SERF atomic magnetometer. Lastly, the data acquisition system was used to process the data. The atom source of the apparatus was K-Rb-Ne. The ratio of potassium atoms to rubidium atoms was approximately 1:70. The alkali metal atomic gas cell was a spherical quartz glass cell with a negligible wall thickness and an external diameter of 10 *mm*. The internal pressure and the working temperature of the vapor cell were 3.5 *atmos* and 200 °C, respectively. A total of three layers of magnetic shield tubes were used to provide a very weak magnetic environment for the SERF magnetometer; the two outer layers were permalloy (1*J*85) and the inner layer was manganese zinc ferrite. The system sampling rate was set to 200 *Hz*.

B. NOISE REDUCTION PROCEDURE

As already mentioned, in this work, we improve the sensitivity of a SERF magnetometer using a method based on the MGGP model of the SERF magnetometer noise. In the experiment, we first calibrated the scale coefficient of the SERF atomic magnetometer following the steps shown in Fig. 4. Ten calibration signals expressed as $S_{in} = B_{cal}\cos(2\pi f_{cal}t)$ were fed to the SERF atomic magnetometer input, where B_{cal} denoted the amplitude of the oscillating magnetic field, and its value was 0.0972 nT, and f denoted the frequency of the oscillating magnetic field. The frequencies of the ten input signals and their corresponding magnetometer output signals are shown in Table 1.

Fitting the amplitude-frequency response by (6), we obtained the values of A, B and C, and they were 3.94×10^4, 22.17 and 20.51, respectively. Therefore, the scale coefficient was $K(f) = 405.35/\left(\sqrt{f^2+22.17^2}+20.51\right)(V/nT)$. The normalized frequency-response function is shown in Fig. 6.

In the experiments, the MGGP tool software 'gptips2' was used. The 'gptips2' is a program package for the determination of the relationships between data which are then represented as functions. The MGGP parameters are presented in Table 2. There were two termination criterions for the MGGP method, achievement of the pre-defined fitness value, and achievement of the pre-specified number of generations. In the experiment, many MGGP models were developed, and the best one among them was chosen based on the fitness function value. The structure of the best MGGP model is defined by (8).

$$\begin{aligned} Y = {} & 2.036\times x_1 - 2.503\times x_2 - 4.99\times_4 - 1.701\times\exp(x_1) \\ & +2.842\times\exp(x_2)+3.084\times\exp(x_4)-1.701\times\sin(x_3) \\ & +11.95\times x_3^4\times x_4^4+1.973\times\left(x_1^2+\cos(x_4)\right)\times\sqrt{x_3+x_4} \\ & -1.701\times x_1^2\times x_3+0.6244\times\sqrt{\cos(x_1+2\times x_2)}-5.67 \end{aligned} \tag{8}$$

In (8), x_i denotes the noise at the time moment $(t-i)$, $i = 1, 2, 3, 4$, and Y denotes the corresponding output of the MGGP model. The magnetometer output signals before and after optimization are shown in Fig. 7. The original data is represented by the blue line in Fig. 7, and it was obtained by recording the magnetometer output for about 370 *s*. The shape

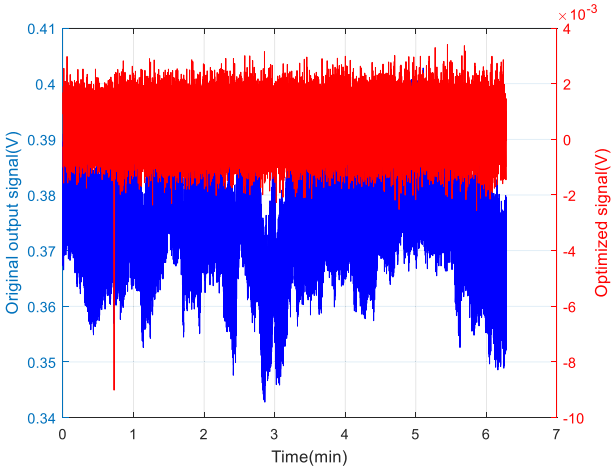

FIGURE 7. The magnetometer output signals before and after optimization.

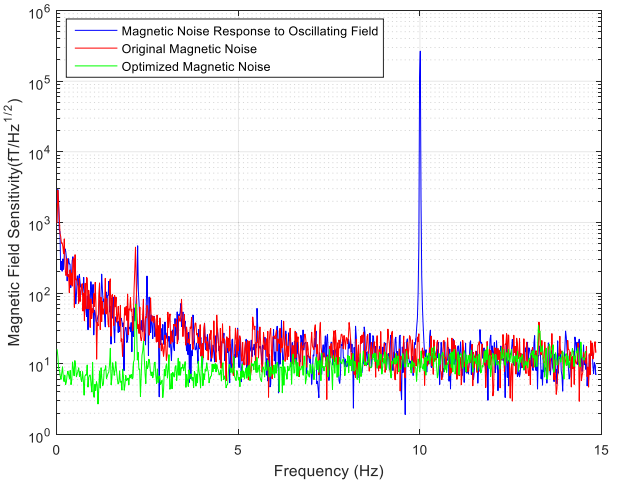

FIGURE 8. The comparison of sensitivity before and after noise reduction.

TABLE 3. The sensitivity comparison at 1 *Hz*, 2 *Hz*, 3 *Hz*, 4 *Hz*, and 5 *Hz*.

Frequency(Hz)	1	2	3	4	5
Original sensitivity($fT/\sqrt{Hz}$)	53.4	32.84	25.52	18.22	15.27
Optimized sensitivity($fT/\sqrt{Hz}$)	3.772	6.937	9.240	9.643	5.893

and the value of the line indicate that the original magnetometer output signal contained a bias and drifts slowly over time. The red curve in Fig. 7 represents the magnetometer output signal optimized by the proposed method. In Fig. 7 it can be seen that in the optimized signal, the noise was obviously reduced, and the signal bias and slow drift were also removed with time, indicating the effectiveness of the proposed method.

C. EXPERIMENTAL RESULTS ANALYSIS

The magnetic field sensitivity data were obtained by recording the magnetometer output for about 100 *s*, and then performing a fast Fourier transform (FFT) without windowing, and calculating rms amplitudes in 15-*Hz* bins. The comparison of sensitivity before and after noise reduction is shown in Fig. 8, where blue curve denotes the noise of the magnetometer response to a 10-*Hz* oscillating magnetic field, the red line represents the magnetic noise of the original source signal of the magnetometer, and green curve shows the magnetic noise after the optimization. The sensitivity comparison at 1 *Hz*, 2 *Hz*, 3 *Hz*, 4 *Hz*, and 5 *Hz* is shown in Table 3.

The experimental results indicate that our method for improving the SERF magnetometer sensitivity achieved good results. In the low-frequency band, especially when the frequency was lower than 10 Hz, the sensitivity of the magnetometer was greatly improved; specifically, at 1 Hz, the magnetometer sensitivity increased by 13 times.

The implementation of the proposed method is very simple and does not require any hardware modification of the SERF magnetometer. Only a laptop with 4G memory is needed, and the user does not need to have any prior knowledge about the noise of the SERF magnetometer. However, the proposed method has some shortcomings. As already mentioned, the model predicts the noise in the SERF atomic magnetometer output signal, and if the prediction lasts too long, the predicted data can be inaccurate. Therefore, it is recommended to conduct measurement for only a few hundred seconds. In addition, although a larger amount of data can make the model more accurate, it also increases model complexity.

IV. CONCLUSION

The SERF magnetometer sensitivity is a very important parameter in the measurement of the magnetic field. In this study, a new method for noise reduction based on the MGGP algorithm is proposed. The MGGP algorithm is employed to model the nonlinear and random characteristics of the SERF magnetometer noise. The experimental results indicate that the proposed method improves the sensitivity of the SERF magnetometer by 13 times at 1 *Hz*. Therefore, the proposed method can significantly reduce the noise and improve the sensitivity of the SERF atomic magnetometer, and consequently improve the accuracy of the magnetic field measurement system. Since, high sensitivity is a characteristic of a SERF atomic magnetometer, modeling of the SERF atomic magnetometer noise is particularly important for the measurement of the magnetic field. The proposed method achieves excellent performance, especially in nonlinear modeling problems, which are very common in practice. Therefore, the proposed method has a wide range of applications.

The proposed method has some limitations, such as poor universality of a model established by the proposed method. In other words, a model established for one magnetometer may not be applicable to another magnetometer. However, the proposed method itself has strong universality. Therefore, we could overcome this problem by modeling specific device by this method before use it.

REFERENCES

[1] C. N. Johnson, P. D. D. Schwindt, and M. Weisend, "Multi-sensor magnetoencephalography with atomic magnetometers," *Phys. Med. Biol.*, vol. 58, no. 17, p. 6065, 2013.

[2] R. Wyllie, M. Kauer, G. S. Smetana, R. Wakai, and T. G. Walker, "Magnetocardiography with a modular spin-exchange relaxation-free atomic magnetometer array," *Phys. Med. Biol.*, vol. 57, no. 9, p. 2619, 2012.

[3] J. M. Brown, "A new limit on Lorentz-and CPT-violating neutron spin interactions using a K-^{3}He comagnetometer," Ph.D. dissertation, Princeton Univ., Princeton, NJ, USA, 2011.

[4] I. Hrvoic, G. M. Hollyer, and P. J. G. S. T. P. Eng, "Brief review of quantum magnetometers," 2005.

[5] R. Stolz, V. Zakosarenko, M. Schulz, A. Chwala, L. Fritzsch, H.-G. Meyer, and E. O. Köstlin, "Magnetic full-tensor SQUID gradiometer system for geophysical applications," *Lead. Edge*, vol. 25, no. 2, pp. 178–180, 2006.

[6] W. Quan, Y. Li, and B. Liu, "Simultaneous measurement of magnetic field and inertia based on hybrid optical pumping," *Europhys. Lett.*, vol. 110, no. 6, 2015, Art. no. 60002.

[7] S. J. Seltzer, *Developments in Alkali-Metal Atomic Magnetometry*. Princeton, NJ, USA: Princeton Univ., 2008.

[8] V. Shah, S. Knappe, P. D. D. Schwindt, and J. Kitching, "Subpicotesla atomic magnetometry with a microfabricated vapour cell," *Nature Photon.*, vol. 1, no. 11, pp. 649–652, Nov. 2007.

[9] T. W. Kornack, "A test of CPT and Lorentz symmetry using a K-^{3}He comagnetometer," Ph.D. dissetrtation, Princeton Univ., Princeton, NJ, USA, 2005.

[10] I. Savukov and T. Karaulanov, "Multi-flux-transformer MRI detection with an atomic magnetometer," *J. Magn. Reson.*, vol. 249, pp. 49–52, Dec. 2014.

[11] K. Kim, S. Begus, H. Xia, S.-K. Lee, V. Jazbinsek, Z. Trontelj, and M. V. Romalis, "Multi-channel atomic magnetometer for magnetoencephalography: A configuration study," *NeuroImage*, vol. 89, pp. 143–151, Apr. 2014.

[12] H. B. Dang, A. C. Maloof, and M. V. Romalis, "Ultrahigh sensitivity magnetic field and magnetization measurements with an atomic magnetometer," *Appl. Phys. Lett.*, vol. 97, no. 15, p. 151110, Oct. 2010.

[13] T. W. Kornack, S. J. Smullin, S.-K. Lee, and M. V. Romalis, "A low-noise ferrite magnetic shield," *Appl. Phys. Lett.*, vol. 90, no. 22, 2007, Art. no. 223501.

[14] J. Fang, T. Wang, W. Quan, H. Yuan, H. Zhang, Y. Li, and S. Zou, "*In situ* magnetic compensation for potassium spin-exchange relaxation-free magnetometer considering probe beam pumping effect," *Rev. Sci. Instrum.*, vol. 85, no. 6, 2014, Art. no. 063108.

[15] F. Jian-Cheng, W. Tao, Z. Hong, L. Yang, and C. Hong-Wei, "*In-situ* measurement of magnetic field gradient in a magnetic shield by a spin-exchange relaxation-free magnetometer," *Chin. Phys. B*, vol. 24, no. 6, 2015, Art. no. 060702.

[16] R. J. Abrahart, F. Anctil, P. Coulibaly, C. W. Dawson, N. J. Mount, L. M. See, A. Y. Shamseldin, D. P. Solomatine, E. Toth, and R. L. Wilby, "Two decades of anarchy? Emerging themes and outstanding challenges for neural network river forecasting," *Prog. Phys. Geography, Earth Environ.*, vol. 36, no. 4, pp. 480–513, 2012.

[17] L. Jianli, J. Feng, F. Jiancheng, and C. Junchao, "Temperature error modeling of RLG based on neural network optimized by PSO and regularization," *IEEE Sensors J.*, vol. 14, no. 3, pp. 912–919, Mar. 2014.

[18] T. L. Xu, "Seamless INS/GPS integration based on support vector machines," *Appl. Mech. Mater.*, vols. 336–338, pp. 277–280, Jul. 2013.

[19] Q. Liu, B. Han, J.-N. Xu, and M. Wu, "Random drift modeling for MEMS gyroscope based on lifting wavelet and wavelet neural network," in *Proc. Int. Conf. Electr. Inf.Control Eng.*, Apr. 2011, pp. 3454–3456.

[20] W. Quan, L. Lv, and B. Liu, "Modeling and optimizing of the random atomic spin gyroscope drift based on the atomic spin gyroscope," *Rev. Sci. Instrum.*, vol. 85, no. 11, 2014, Art. no. 113104.

[21] W. Quan, G. Li, Z. Fang, Y. Zhai, X. Li, and F. Liu, "Locking distributed feedback laser diode frequency to gas absorption lines based on genetic programming," *Proc. SPIE*, vol. 56, no. 1, 2017, Art. no. 016106.

[22] D. D. Searson, "GPTIPS: Genetic programming and symbolic regression for MATLAB," Newcastle Univ., Newcastle upon Tyne, U.K., 2009.

[23] S. Vitale, G. A. Prodi, and M. Cerdonio, "Thermal magnetic noise in RF SQUIDS coupled to ferromagnetic cores," *J. Appl. Phys.*, vol. 65, no. 5, pp. 2130–2136, 1989.

[24] J. R. Koza and R. Poli, "A genetic programming tutorial," in *Introductory Tutorials in Optimisation, Decision Support*, vol. 8. 2003, pp. 1–40.

[25] P. Bahrami, P. Kazemi, S. Mahdavi, and H. Ghobadi, "A novel approach for modeling and optimization of surfactant/polymer flooding based on genetic programming evolutionary algorithm," *Fuel*, vol. 179, pp. 289–298, Sep. 2016.

[26] M.-I. Kim and P. Zou, "Modeling of drilling forces based on twist drill point angles using multigene genetic programming," *Math. Problems Eng.*, vol. 2016, Jan. 2016, Art. no. 6749182.

[27] M. Quade, M. Abel, K. Shafi, R. K. Niven, and B. R. Noack, "Prediction of dynamical systems by symbolic regression," *Phys. Rev. E, Stat. Phys. Plasmas Fluids Relat. Interdiscip. Top.*, vol. 94, no. 1, 2016, Art. no. 012214.

[28] R. Li, W. Quan, W. Fan, L. Xing, Z. Wang, Y. Zhai, and J. Fang, "A dual-axis, high-sensitivity atomic magnetometer," *Chin. Phys. B*, vol. 26, no. 12, 2017, Art. no. 120702.

[29] I. K. Kominis, T. W. Kornack, J. C. Allred, and M. V. Romalis, "A subfemtotesla multichannel atomic magnetometer," *Nature*, vol. 422, no. 6932, pp. 596–599, 2003.

WEI QUAN received the Ph.D. degree from Beihang University, in 2008. He is currently a Professor with the School of Instrumentation and Optoelectronic Engineering, Beihang University. His research interests include celestial navigation and the recently developed atomic inertial sensors based on alkali-metal vapor cell.

FENG LIU received the B.S. degree in control science and engineering from Shandong University, China, in 2014. He is currently pursuing the Ph.D. degree with the School of Instrumentation and Optoelectronic Engineering, Beihang University. His research interests include the magnetic response of atomic magnetometer and comagnetometer operated in the spin-exchange relaxation-free regime.

WENFENG FAN received the B.S. degree in mechanical engineering from Shandong University, China, in 2012. He is currently pursuing the Ph.D. degree with the School of Instrumentation and Optoelectronic Engineering, Beihang University. His research interests include the magnetic response of atomic magnetometer and comagnetometer operated in the spin-exchange relaxation-free regime.